Mon. Not. R. astr. Soc. (1970) **150**, 253–270.

MAPS OF THE DISTRIBUTION OF POLARIZATION IN FIVE RADIO SOURCES AT 21·1-CM WAVELENGTH

J. E. Baldwin, J. E. Jennings, J. R. Shakeshaft, P. J. Warner, D. M. A. Wilson and M. C. H. Wright

(Received 1970 July 2)

SUMMARY

The method of operation of the recently completed Half-Mile radio telescope at Cambridge for the mapping of the linear polarization of continuum sources is described. Polarization maps at λ 21·1 cm are presented for five sources: 3C 10 (Tycho's SN), 111, 144 (Crab Nebula), 452, 461 (Cas A). In addition 3C 286 and 405 (Cyg A) have been observed.

1. INTRODUCTION

Many studies have been made in recent years of the net linear polarization of radio sources and its variation with wavelength but it is likely that our understanding of sources will be significantly advanced by maps of their polarization distributions at different wavelengths with resolving power adequate to reveal the magnetic field structure. Except in a few cases, such as Centaurus A (e.g. Cooper, Price & Cole 1965), interferometric methods (Morris, Radhakrishnan & Seielstad 1964) are necessary to obtain the resolution. Several papers (e.g. Seielstad & Weiler 1968; Kronberg & Conway 1970) describing one-dimensional aperture synthesis have already been published and two-dimensional aperture synthesis is now being carried out at various observatories (e.g. Seielstad 1969a; Fomalont 1970). During the past four years a new radio telescope, the Half-Mile telescope, has been under construction and in operation at the Mullard Radio Astronomy Observatory, one of the purposes of which is to carry out such mapping in the continuum at a wavelength of 21·1 cm. This paper describes the instrument briefly and the first results of its application to the polarization mapping of sources. Section 2 describes the telescope, Section 3 the method of measurement and Section 4 the observations. In Section 5 the reduction of the data is discussed and in Section 6 the results are presented.

2. THE HALF-MILE TELESCOPE

The Half-Mile telescope consists of a two-element interferometer on an east–west line and is designed to operate as an earth rotation synthesis instrument at frequencies near 1420 MHz, in a manner closely similar to the One-Mile telescope (Elsmore, Kenderdine & Ryle 1966). Each element is an equatorially mounted paraboloidal reflector with a diameter of 9 m and a focal ratio 0·433. One of the reflectors is at the west end of the rail track of the One-Mile telescope and the other is on a carriage which may be moved to positions along the track to the east. A range of spacings from 9·4 m (45 λ) to 732 m (3464 λ) is then available, giving a maximum resolution of 47″ to half-power points. For reasons of economy

in the construction, and since in any case the resolving power of systems of this type falls rapidly at lower declinations, the lower limit of declination was chosen to be 20°.

At the focus of each reflector is a pair of orthogonal dipoles in a circular waveguide. These are aligned to give two pairs of parallel and two pairs of orthogonal interferometer feeds. Two 1420 MHz degenerate parametric amplifiers are installed at each focus and the R. F. signals pass via air-spaced flexible coaxial cable to mixers and I.F. amplifiers at the base of each reflector. The coherent local oscillator signal is derived from a 91·65 MHz temperature controlled crystal in the central laboratory and transmitted at 366·6 MHz by equal cables, buried as far as is possible, to each aerial where multiplication to 1466·4 MHz takes place. No attempt is made to keep the pumps for the parametric amplifiers coherent and the effective system noise is 220° K.

The 45 MHz I.F. signals are transmitted by buried coaxial cables to the central laboratory, where they pass through two independent path-compensating and fringe-slowing systems, each as described by Elsmore *et al.* (1966). After further amplification the four signals are split in a hybrid network to give inputs in phase and in antiphase for four pairs of cosine and sine phase-switching receivers with bandwidths 4 MHz, and a multi-channel spectrometer. The outputs of three of the four pairs of cosine and sine receivers are sampled cyclically every 30 s so that cosine and sine outputs are recorded digitally on paper tape every 10 s. This sampling, the switching of the path-compensating and fringe-slowing systems, and the tracking of the reflectors, are controlled automatically by a five-track paper tape reader synchronized to a sidereal clock.

3. MEASUREMENT OF POLARIZATION

The response of a phase-switching interferometer to a source of partially polarized radiation has been discussed by Morris *et al.* (1964) using the Stokes parameters I, Q, U and V, defined in terms of the complex visibility functions for the corresponding brightness distributions over the source. In the present paper the quantities Q and U are defined with respect to position angle 0°, so that an incident wave, linearly polarized with its electric vector in position angle 0°, would have Q positive and U zero.

If the dipoles in both the east (E) and west (W) antennas are aligned at position angles 0° and 90° then the four available outputs of the interferometer are

$$\mathrm{E_0W_0} \propto I+Q$$

$$\mathrm{E_{90}W_{90}} \propto I-Q$$

$$\mathrm{E_0W_{90}} \propto U+jV$$

$$\mathrm{E_{90}W_0} \propto U-jV$$

where $\mathrm{E_0\ W_{90}}$, for example, is the output from the dipole at position angle 0° in the east feed and the dipole at position angle 90° in the west feed. The arrangement of receivers enables any three of these outputs to be recorded as described in Section 2.

If the radiation has no component of circular polarization, i.e. $V = 0$, then I, Q and U may, in principle, be deduced from, say, the first three combinations.

In practice, although it was assumed that $V = 0$, the net polarizations of the sources studied in the present work were small so that I is much greater than Q and the measurement of Q by subtraction of the outputs $(E_0W_0 - E_{90}W_{90})$ was not sufficiently accurate. Further observations were therefore made with the dipoles in position angles 45° and 135° giving the four outputs

$$E_{45}W_{45} \propto I + U$$

$$E_{135}W_{135} \propto I - U$$

$$E_{45}W_{135} \propto Q + jV$$

$$E_{135}W_{45} \propto Q - jV$$

so that, if $V = 0$, Q is found directly.

The interpretation of the results obtained with a radio polarimeter is complicated both by the presence of sources of radiation off the axis of the beam and also by the instrumental polarization. Unpolarized sources off the axis of the beam appear to be partially linearly polarized even for perfect paraboloidal reflectors. This well-known effect has been analysed in detail by Kerdemelidis (1966) and for the Half-Mile telescope the predicted linear polarization reaches a maximum, at 66′ arc from the axis of the beam, of 2·7 per cent of the main response. Measurements of the polar diagrams of the pairs of crossed dipoles were made by means of drift scans of the sources Cas A and Cyg A and the agreement with theory was found to be satisfactory. For sources at the centre of the beam, and less than 10′ arc in angular extent, the apparent polarization due to this is less than 0·2 per cent of the unpolarized flux density.

Imperfections in the reflectors and feeds can give rise to spurious polarization even on the axis of the beam. This effect is most easily measured by observations of an intense unpolarized source. It was found that, at λ 21·1 cm, Cyg A is effectively unpolarized (see later) and could therefore be used to determine the instrumental polarization.

4. THE OBSERVATIONS

Six sources have been studied in this first series of observations with the Half-Mile telescope in the period December 1968–July 1969. They were selected on account of their high flux density or large angular size and large net polarization. For each source the number of spacings used in the synthesis was such as to minimize the total observing time whilst keeping the grating rings on the map well outside the source. The objects studied and the number of spacings used are given in Table I.

TABLE I

Source	Number of spacings
Cyg A	4
Cas A	8
Tau A	8
3C 10	10
3C 111	4
3C 452	5

In addition the polarization of 3C 286 has been measured although this object cannot be resolved by the present instrument.

The source 3C 295 was observed daily for calibration of the collimation and sensitivity of the instrument. Over the range of spacings available (45 − 3464 λ) 3C 295 may be regarded as an unresolved point source. Its position and flux density were taken as:

$$\left.\begin{aligned}\alpha &= 14^{h}\ 09^{m}\ 33^{s}\cdot 44\\ \delta &= 52^{\circ}\ 26'\ 13''\cdot 60\end{aligned}\right\}\ 1950\cdot 0$$

$$S(1421) = 21\cdot 4\times 10^{-26}\ \mathrm{W\ m^{-2}\ Hz^{-1}}$$

There are, unfortunately, no known small diameter sources which provide a polarized flux adequate for calibration of the outputs derived from the pairs of orthogonal dipoles. Auxiliary dipoles were therefore installed, one at the pole of each reflector, to which correlated CW signals could be fed from the central laboratory. These calibration dipoles were set at angles of 45° relative to the dipoles in the feed and it was possible in this way to measure the relative phase and amplitude of the outputs from the crossed dipoles and the parallel dipoles in the feeds. The characteristics of each of the three independent receiving systems were closely similar across the receiving band so that calibration at a single CW frequency was sufficient to provide the calibration for a continuum source.

No systematic variations in the sensitivity of the instrument were detected during individual calibrations runs on 3C 295, but there were found to be random variations of sensitivity from day to day with a scatter of about ± 5 per cent. The collimation error varied with the temperature of the flexible coaxial cable connecting the movable telescope to the nearest access point to the underground cables, and during this series of observations the temperature effect caused changes of collimation error of up to ± 10°. Although some allowance could be made for these in the reduction, it is likely that phase errors of up to 5° remain in the data. These are believed to be the largest source of error in the final maps.

5. REDUCTION OF THE DATA

Maps of the distribution of the Stokes parameters for each source are produced by Fourier inversion of the appropriate outputs as discussed in Section 3. In order to determine the corrections for instrumental polarization, the sources Cas A and Cyg A were observed at small base-lines so that the sources were unresolved and the output from orthogonal dipoles was therefore the sum of the net polarization of the source and the instrumental polarization. A quadrature component was found for each source, of magnitude (0·5 ± 0·1) per cent of the total intensity. The fact that the sign of this component was the same for both the $E_0\ W_{90}$ and $E_{90}\ W_0$ systems proved it to be, at least in part, an instrumental effect associated with the feeds. Small in-phase components were also found but of opposite signs for the two sources, indicating that one or both of the sources have a small net linear polarization. For the reasons given below we have, in fact, assumed that Cyg A is unpolarized at λ 21·1 cm. The apparent polarization for this source is then that of the instrument and is expressed as a percentage of the *I* value in Table II.

TABLE II

System	Instrumental polarization (% of I)
E_0 W_{90}	$0{\cdot}1 + j\,0{\cdot}5$
E_{90} W_0	$1{\cdot}7 + j\,0{\cdot}5$
E_{135} W_{45}	$0{\cdot}16 + j\,0{\cdot}26$

The signs indicate the phase with respect to that of the CW reference signal.

Our assumption can be justified by the following:

(i) Cas A then has a linear polarization $Q = (-0{\cdot}15 \pm 0{\cdot}07)$ per cent which agrees within the limits of error with the value, at the same wavelength, quoted by Seielstad & Weiler (1968), viz. $(0{\cdot}11 \pm 0{\cdot}07)$ per cent in p.a. $116° \pm 45°$; and

(ii) 3C 48 and 3C 295, observed with long integration times, have no polarization greater than 0·5 per cent. Bologna, McClain & Sloanaker (1969) give values, at λ 21·2 cm, of $(0{\cdot}1 \pm 0{\cdot}6)$ per cent and $(0{\cdot}0 \pm 0{\cdot}5)$ per cent respectively.

Use of the Stokes parameters for specifying the polarization enables the instrumental correction to be applied by direct subtraction. Because of the linearity of the Fourier transform the correction can equally well be applied to the maps themselves. For sources with small percentage polarization it is sufficiently accurate to subtract the appropriate fraction of the response obtained with any of the systems using parallel dipoles.

The effects of correction for instrumental polarization are illustrated in Fig. 1 where (a) shows the contour map of I–U for Cygnus A, as obtained with parallel dipoles in a position angle of 135°, (b) is the uncorrected map of the polarized component as obtained with orthogonal dipoles E_0 W_{90}, while (c) gives the map of (b) as corrected for instrumental polarization. Although the correction procedure is based on the assumption that there is no polarization from the source as a whole, it can be seen that the same is true for the individual components. This provides some confirmation of the assumption of zero net polarization in Cyg A. The residual contours on Fig. 1(c) are 0·1 per cent of the total intensity and are believed to be due to instrumental effects occurring at transit.

6. RESULTS AND DISCUSSION

Results for the individual sources are presented in this section. 1950·0 coordinates are used throughout for the maps. The zero level in each case is arbitrary and has been established by averaging regions remote from the source. The contours are drawn at equal intervals, with the lowest contour at a full interval from the zero level. In a few cases extra contours at half the normal interval have been inserted to show detail; these are drawn as thin lines. Negative contours are shown as dashed lines.

The maps of Cyg A, 3C 10 and the Crab Nebula have equal coordinate scales in right ascension and declination. Those of 3C 111, 3C 452 and Cas A have the scale in declination compressed by sin δ so that the synthesized beam is circular. These latter are noted in the captions as being in ' aerial coordinates '.

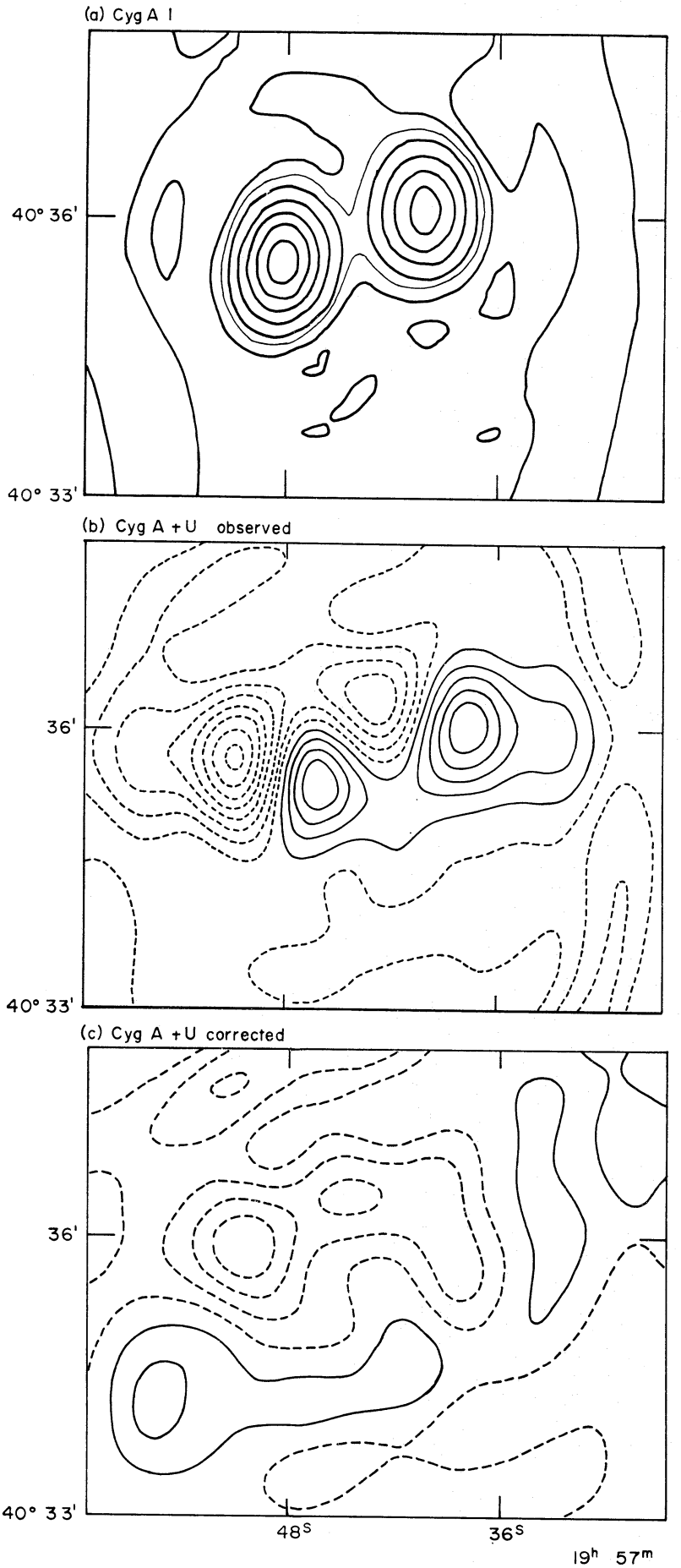

FIG. 1.

6.1 3C 10 (*Tycho's Supernova*)

At the full resolution, obtained by observations at ten spacings, the peak signal-to-noise ratio on the maps of Q and U was only about unity. The signal-to-noise ratio was therefore improved by omitting the four largest spacings from the synthesis, with a consequent beam broadening to $77'' \times 85''$ arc between half-power points. The resulting maps, on which the r.m.s. noise level is 2×10^{-28} W m^{-2} Hz^{-1} (beam area)$^{-1}$, are shown in Figs 2(b) and (c). East–west strip distributions prepared from these maps agree within the limits of error with those by Seielstad & Weiler (1968).

The maps of Q and U have been combined in Fig. 2(a) to give the vectors of the polarized flux density (parallel to the directions of the electric vector) superposed on contours of the total intensity at the same resolution. A grating response due to the nearby source 3C 11·1 has been removed from this figure.

Baldwin (1967) has already presented a map of the total intensity at λ 21·3 cm with much higher resolution ($21'' \times 23''$ arc) which shows a symmetrical ring of emission with a sharp outer edge and a remarkably low brightness temperature in the centre. The largest features on both the Q and U maps coincide with the ring and are (7 ± 2) per cent of the total intensity in the same region, although a more typical value for the ring is (5 ± 2) per cent. These quoted errors correspond to the r.m.s. noise level, so to a 95 per cent confidence level we can say that nowhere on the ring does the λ 21·1–cm polarization exceed 11 per cent. These values may be compared with the maps of $(I+Q)$ and $(I-Q)$ by Dickel (1969) with a 2′ arc beam at λ 2 cm. There are differences of twice the quoted noise level between these maps, representing a degree of polarization of 30 per cent and implying that there is substantial depolarization at the longer wavelength. Unfortunately the presently available data on the polarization of 3C 10 do not permit any more detailed discussion.

6.2 3C 111

The maps of I, Q and U are shown in Fig. 3 and the information from the Q and U maps has been combined to give the plot of the E field polarization vector superposed on the I map. The latter agrees well with the higher resolution map (of $I+Q$ in fact) at λ 21·3 cm by Mackay (1969). The three main components are distinguishable in Fig. 3(a) and one of them is partially resolved. The r.m.s. noise level on the maps of Q and U is 2×10^{-28} W m^{-2} Hz^{-1} (beam area)$^{-1}$ and is mainly responsible for the vectors lying outside the source in Fig. 3(a). The distribution of polarization is consistent with the one-dimensional distribution obtained by Seielstad & Weiler (1968) at λ 21·1 cm. The values for percentage

---

FIG. 1. 3C 405 (*Cygnus A*). (*a*) *Contours of I–U. Contour interval* 128×10^{-26} *W m*$^{-2}$ *Hz*$^{-1}$ *(beam area)*$^{-1}$. (*b*) *Contours of U (from* E_0 W_{90}*)* before *correction for instrumental polarization. Contour interval* $0{\cdot}44 \times 10^{-26}$ *W m*$^{-2}$ *Hz*$^{-1}$ *(beam area)*$^{-1}$. (*c*) *Contours of U (from* E_0 W_{90}*)* after *correction for instrumental polarization. Contour interval* $0{\cdot}22 \times 10^{-26}$ *W m*$^{-2}$ *Hz*$^{-1}$.

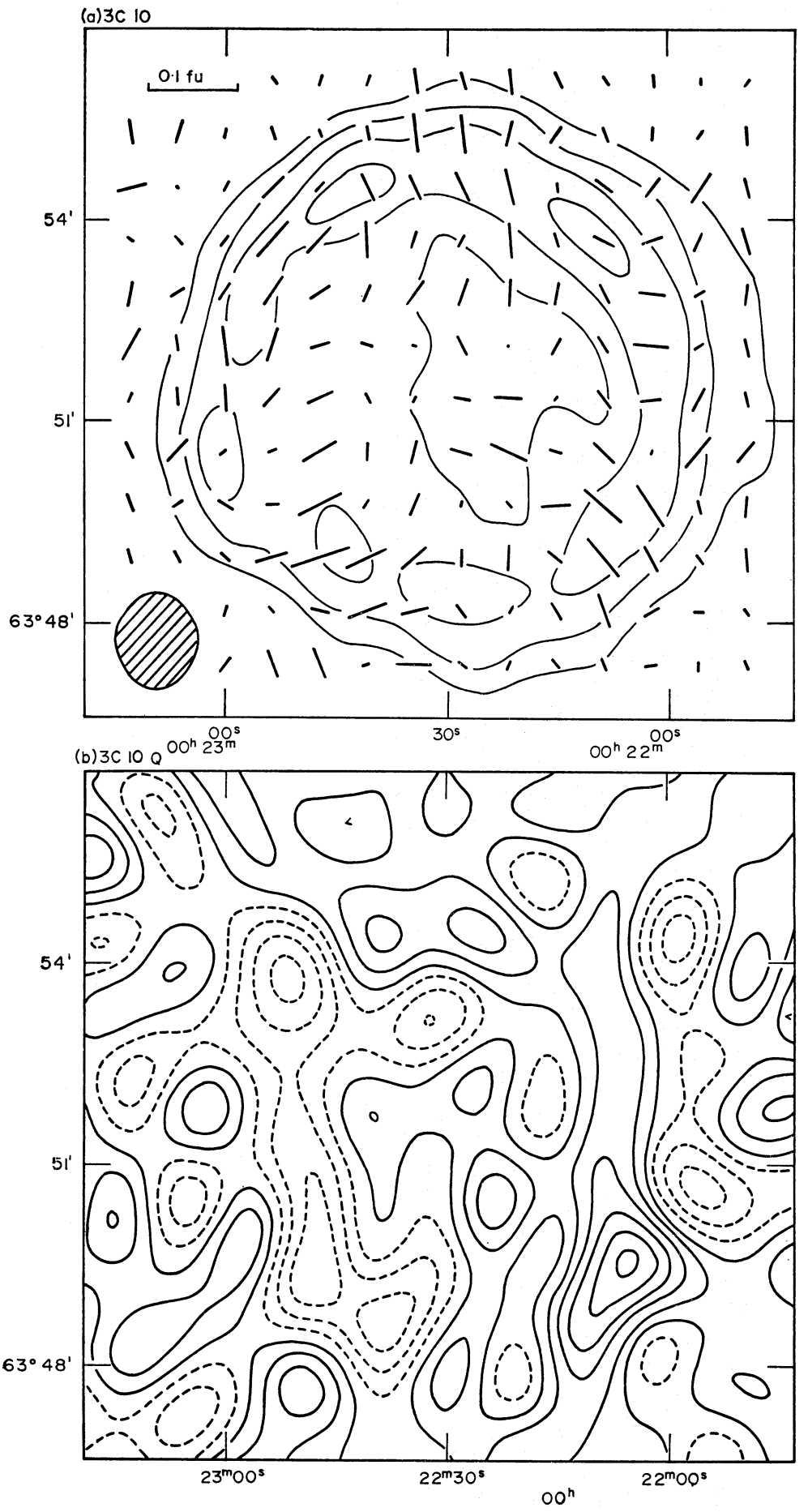

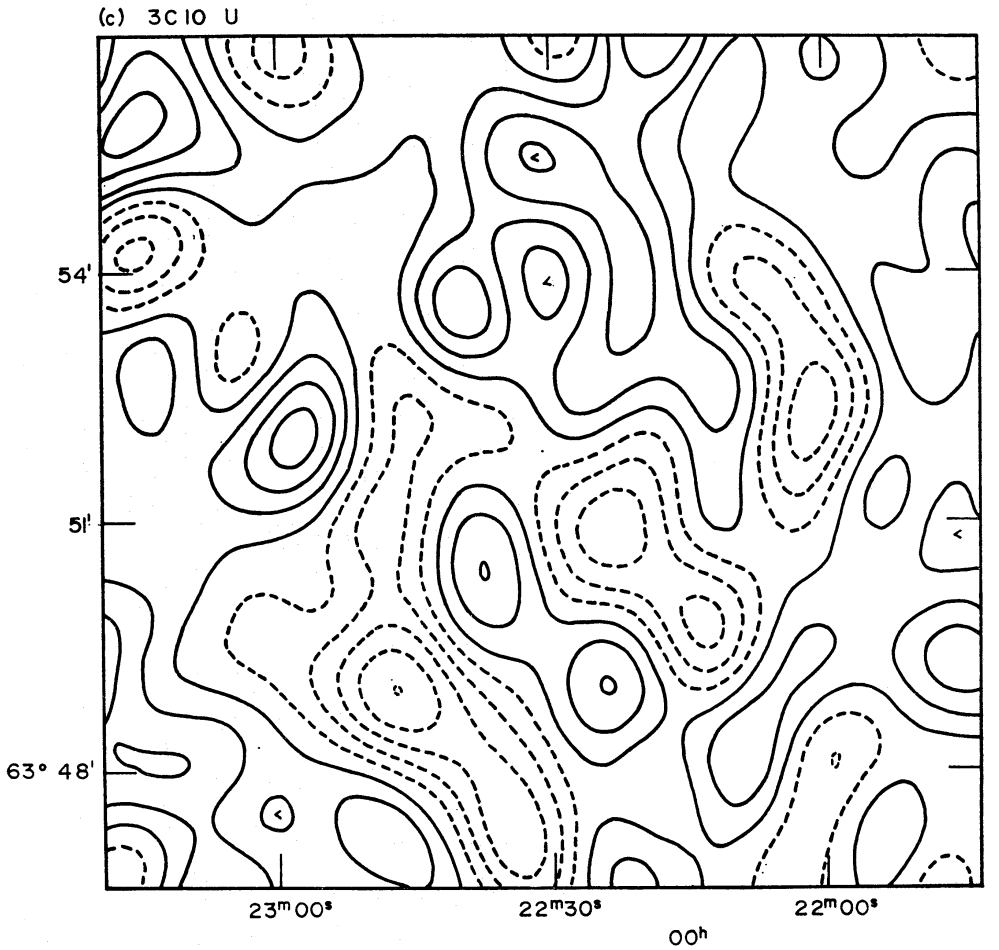

FIG 2. 3C 10 (*Tycho's SN*). (*a*) *Vectors of polarized flux superposed on contours of the total intensity. The inset, marked* 0·1 *fu, is the length of a vector representing a polarized flux density of* 10^{-27} *W m*$^{-2}$ *Hz*$^{-1}$ (*beam area*)$^{-1}$. *The contour interval is* 4×10^{-27} *W m*$^{-2}$ *Hz*$^{-1}$ (*beam area*)$^{-1}$ *and the half-power width of the synthesized beam is indicated by the shaded area.* (*b*) *and* (*c*) *Contours of Q and U respectively. The contour interval is* $1{\cdot}3 \times 10^{-28}$ *W m*$^{-2}$ *Hz*$^{-1}$ (*beam area*)$^{-1}$. *The r.m.s. noise level is* $1\frac{1}{2}$ *contours.*

polarization and position angle for separate components of 3C 111 are

Right ascension	Polarization (per cent)	Position angle (°)
$04^h\ 14^m\ 55^s$	$9{\cdot}2 \pm 1$	67 ± 3
04 15 00	$4{\cdot}5 \pm 3$	130 ± 30
04 15 06	$6{\cdot}5 \pm 1$	122 ± 10
04 15 09	$5{\cdot}5 \pm 0{\cdot}7$	32 ± 5

The third component is in the inner extension of the north-following peak and, as can be seen from Fig. 3(b), is largely independent of it. It should be noted that the degree of polarization of the individual components approaches the largest values which have been measured in sources comprising a single compact component (e.g. 3C 286). Unfortunately there are no data available for the individual components at other frequencies.

Table III lists values of the net polarization of 3C 111. The agreement between measurements at the same wavelength is evidently satisfactory but the interpretation of the results as a whole is not unambiguous. The simplest interpretation

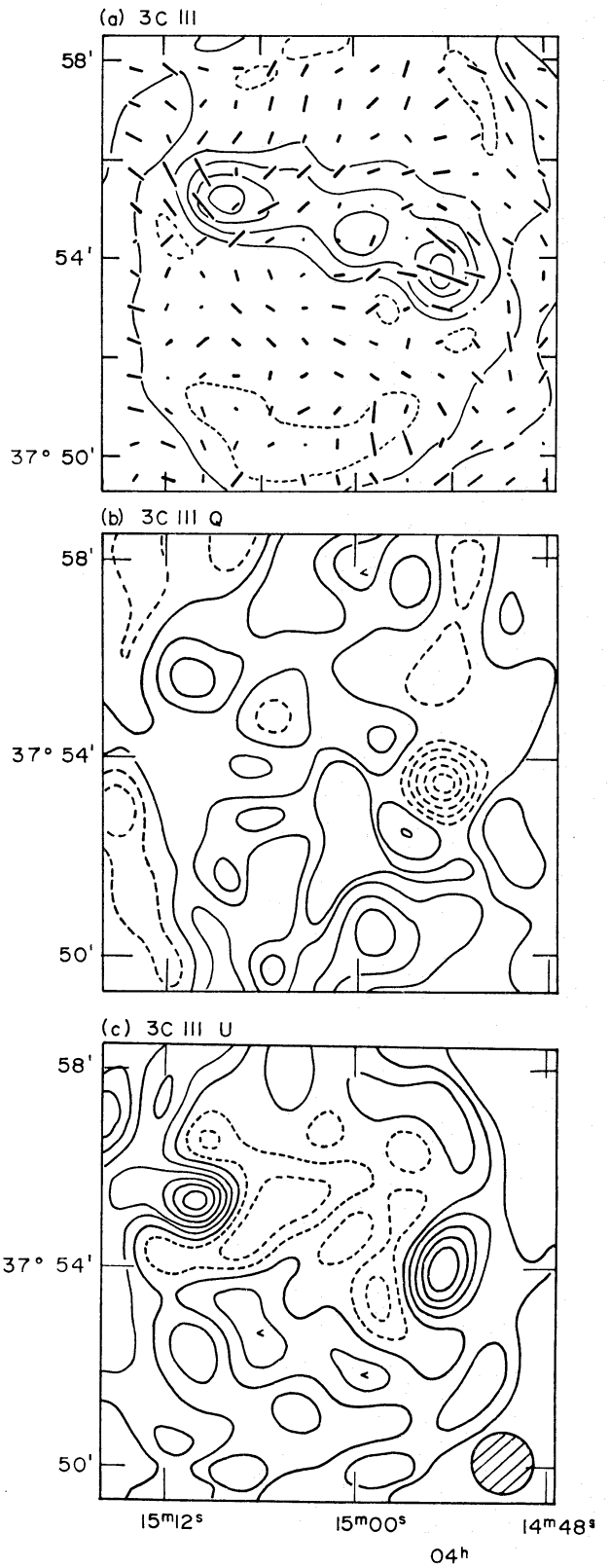

FIG. 3. 3C 111. (*a*) *Vectors of polarized flux superposed on contours of total intensity. The longest vector at the position of the Sp peak represents a polarized flux density of* $0{\cdot}17 \times 10^{-26}$ *W m*$^{-2}$ *Hz*$^{-1}$ *(beam area)*$^{-1}$, *and is* 9 *per cent of the total intensity. The contour interval is* $0{\cdot}7 \times 10^{-26}$ *W m*$^{-2}$ *Hz*$^{-1}$ *(beam area)*$^{-1}$. *Aerial coordinates.* (*b*) *and* (*c*) *Contours of Q and U respectively. The contour interval is* $2{\cdot}6 \times 10^{-28}$ *W m*$^{-2}$ *Hz*$^{-1}$ *(beam area)*$^{-1}$. *Aerial coordinates. The r.m.s. noise level is* 2×10^{-28} *W m*$^{-2}$ *Hz*$^{-1}$ *(beam area)*$^{-1}$.

TABLE III

The net polarization of 3C 111 at different wavelengths

	λ (cm)	Polarization (per cent)	Position angle (°)
Kronberg & Conway (1970)	49·1	1·4±0·2	34±10
Bologna *et al.* (1969)	21·2	1·9±0·6	80± 8
This paper	21·1	1·6±0·3	79± 4
Seielstad & Weiler (1969)	21·1	1·8±0·3	90± 4
Morris & Berge (1964)	18·0	2·1±0·4	120± 8
Morris & Berge (1964)	10·6	3·3±1·8	116±14
Sastry *et al.* (1967)	6	1·3±0·6	131±14

is that the degree of polarization is independent of frequency and the rotation measure is -19 rad m^{-2}. In this case the distribution of intrinsic polarization would be given by the map of Fig. 3(a) with the position angle of all the vectors increased by about 49°. This rotation measure is consistent with the values for other nearby sources (Berge & Seielstad 1967). The existence, however, of comparatively large spectral differences between the components (Mitton 1970) must

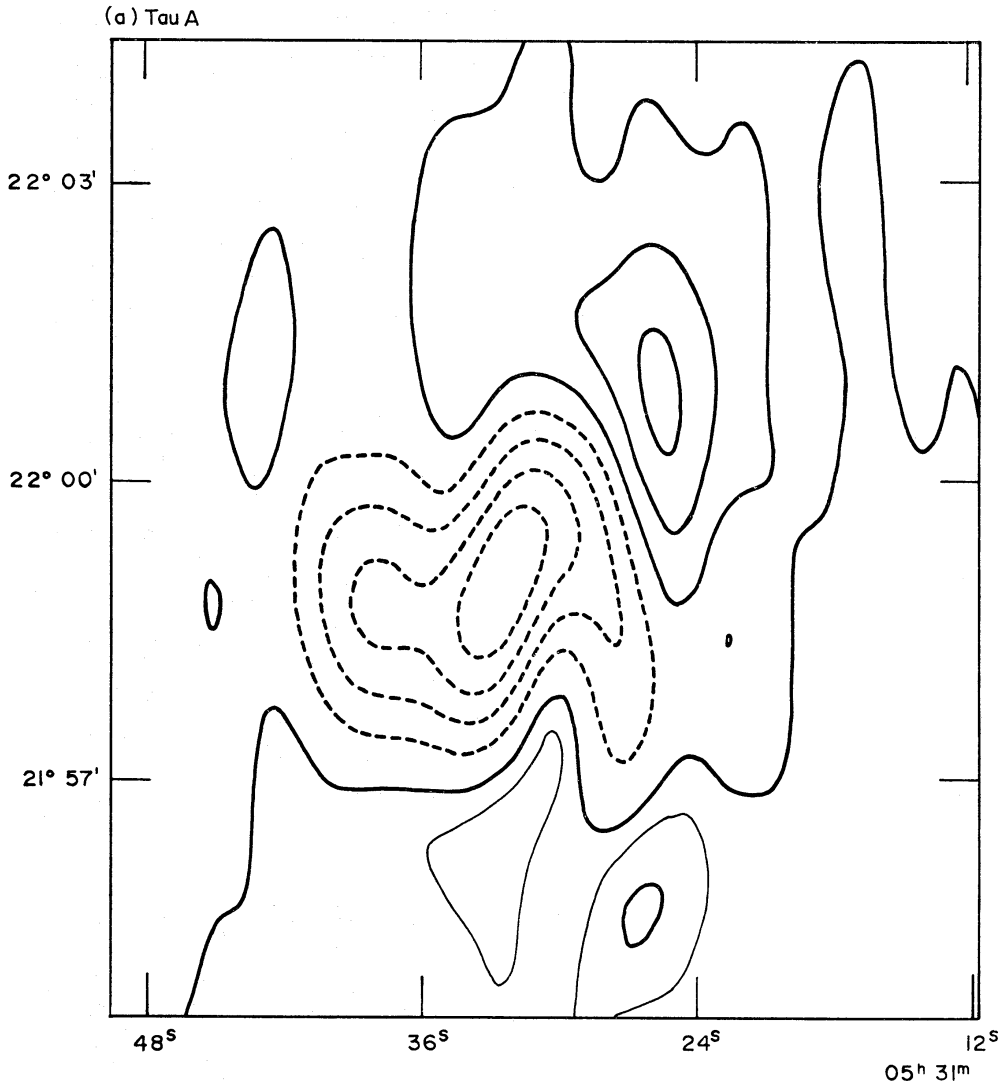

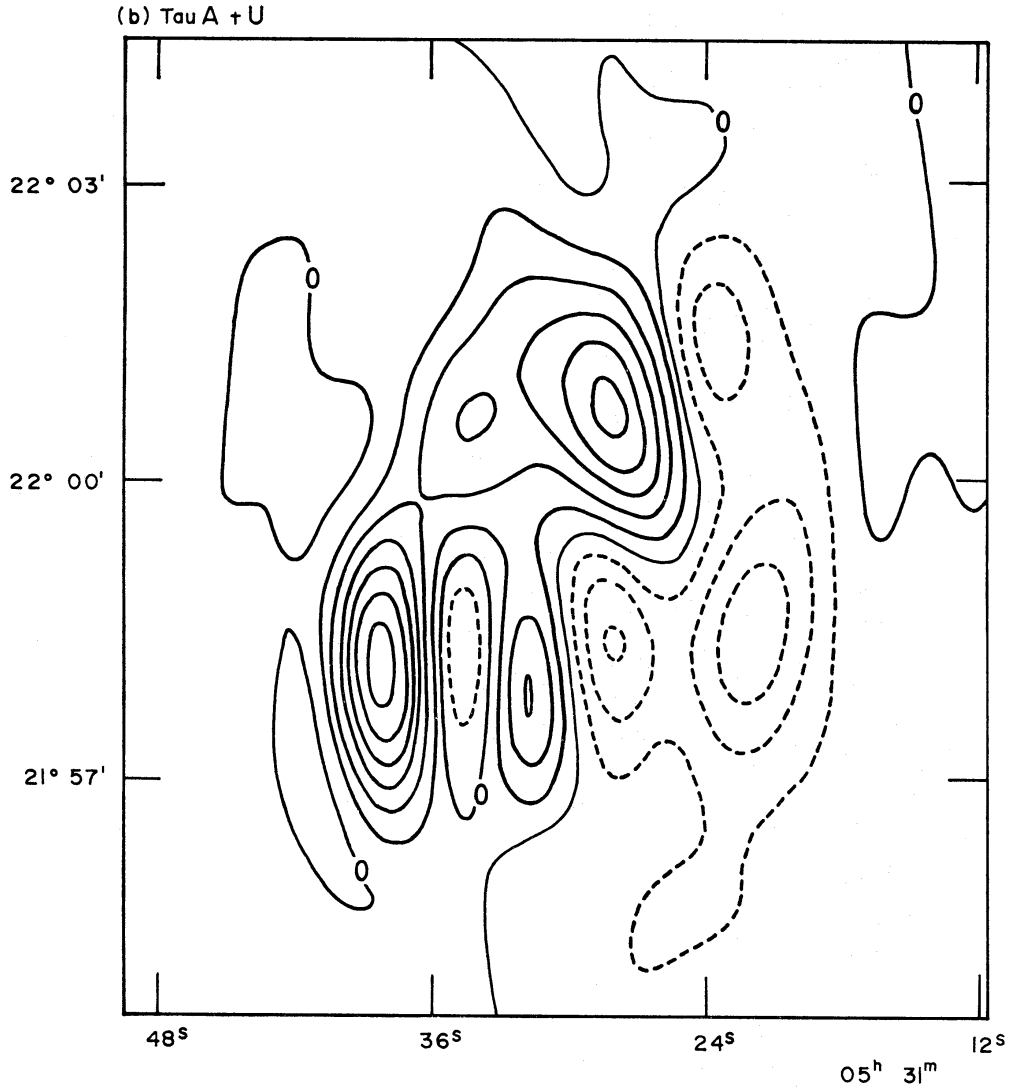

FIG. 4. 3C 144 (*Crab Nebula*). (*a*) *Contours of Q. The contour interval is* $0{\cdot}77 \times 10^{-26}$ *W* m^{-2} *Hz*$^{-1}$ (*beam area*)$^{-1}$. (*b*) *Contours of U. The contour interval is* $0{\cdot}25 \times 10^{-26}$ *W* m^{-2} *Hz*$^{-1}$ (*beam area*)$^{-1}$.

complicate the situation but a detailed treatment is not justifiable until better data are obtained.

6.3 3C 144 (*Crab Nebula*)

The maps of Q and U are shown in Fig. 4 with a resolution of $47'' \times 126''$ arc. They are discussed in detail in the following paper (Wright 1970) and will not be considered further here.

6.4 3C 286

3C 286 is known to be quite strongly linearly polarized at λ 21·1 cm (Morris & Berge 1964) but there has recently been some controversy concerning a possible circularly polarized component. It was therefore included in the observing programme although it cannot be resolved by the Half-Mile telescope.

Q and U have been determined from the outputs E_0 W_{90} and E_{45} W_{135}, the

accuracy being limited by that of the gain calibrations. V has been determined from comparison of the phases of the outputs E_0 W_{90} and E_{90} W_0 as compared with that deduced from the CW calibrations and from observations of 3C 295, assumed to have V zero. The accuracy of measurement of V is limited by residual uncertainties in the geometry of the instrument and the instrumental polarization.

The results are as follows:

$$\left.\begin{aligned} Q &= (8{\cdot}1 \pm 0{\cdot}5) \text{ per cent} \\ U &= (2{\cdot}3 \pm 0{\cdot}3) \text{ per cent} \\ V &= (-0{\cdot}1 \pm 0{\cdot}2) \text{ per cent} \end{aligned}\right\} \text{ at } \lambda\, 21{\cdot}1 \text{ cm}$$

equivalent to a linear polarization

$$p = (8{\cdot}4 \pm 0{\cdot}5) \text{ per cent in p.a. } (35 \pm 2)^\circ \text{ and a circular polarization } (-0{\cdot}1 \pm 0{\cdot}2) \text{ per cent.}$$

These values are in good agreement with those by Morris & Berge (1964), i.e.

$$p = (9{\cdot}3 \pm 0{\cdot}5) \text{ per cent in p.a. } (32 \pm 5)^\circ \text{ at } \lambda\, 21{\cdot}1 \text{ cm.}$$

Biraud (1969) has reported the detection of a circularly polarized component at λ 11·1 cm of $(-2{\cdot}96 \pm 0{\cdot}35)$ per cent, although he advises caution in acceptance of this value because of the lack of symmetry between the two polarizations on the Nançay radio telescope and the large linear polarization of 3C 286. Seielstad (1969b) and Berge & Seielstad (1969), on the other hand, find values for this component not significantly different from zero at wavelengths bracketing λ 11·1 cm, i.e.

$$(-0{\cdot}20 \pm 0{\cdot}26) \text{ per cent at } \lambda\, 21{\cdot}1 \text{ cm}$$

and

$$(-1{\cdot}0 \pm 1{\cdot}0) \text{ per cent at } \lambda\, 3{\cdot}13 \text{ cm.}$$

It can be seen that our value confirms that by Seielstad at λ 21·1 cm.

6.5 3C 452

Fig. 5 shows the maps of I, Q and U. Superposed on the map of I are the polarization vectors derived from the values of Q and U. The source is well resolved along its major axis but unresolved in declination. The I map is in good agreement with the higher resolution map of $(I+Q)$ at λ 21·3 cm by Macdonald, Kenderdine & Neville (1968) and the polarization distribution is consistent with that found from the fan-beam observations by Seielstad & Weiler (1968).

Table IV lists values of the net polarization of 3C 452 and it can be seen that measurements at similar wavelengths agree. Seielstad & Weiler (1969) have already shown from comparison of their results at λ 21·1 cm with those of Seielstad (1967) at λ 10·6 cm that the net depolarization at the longer wavelength is attributable to rapid depolarization of the leading component whereas the polarization of the following component remains effectively constant. The present results (Table V) confirm the depolarization of the preceding component but indicate that substantially larger values of percentage polarization are found for the following component when higher resolution is used.

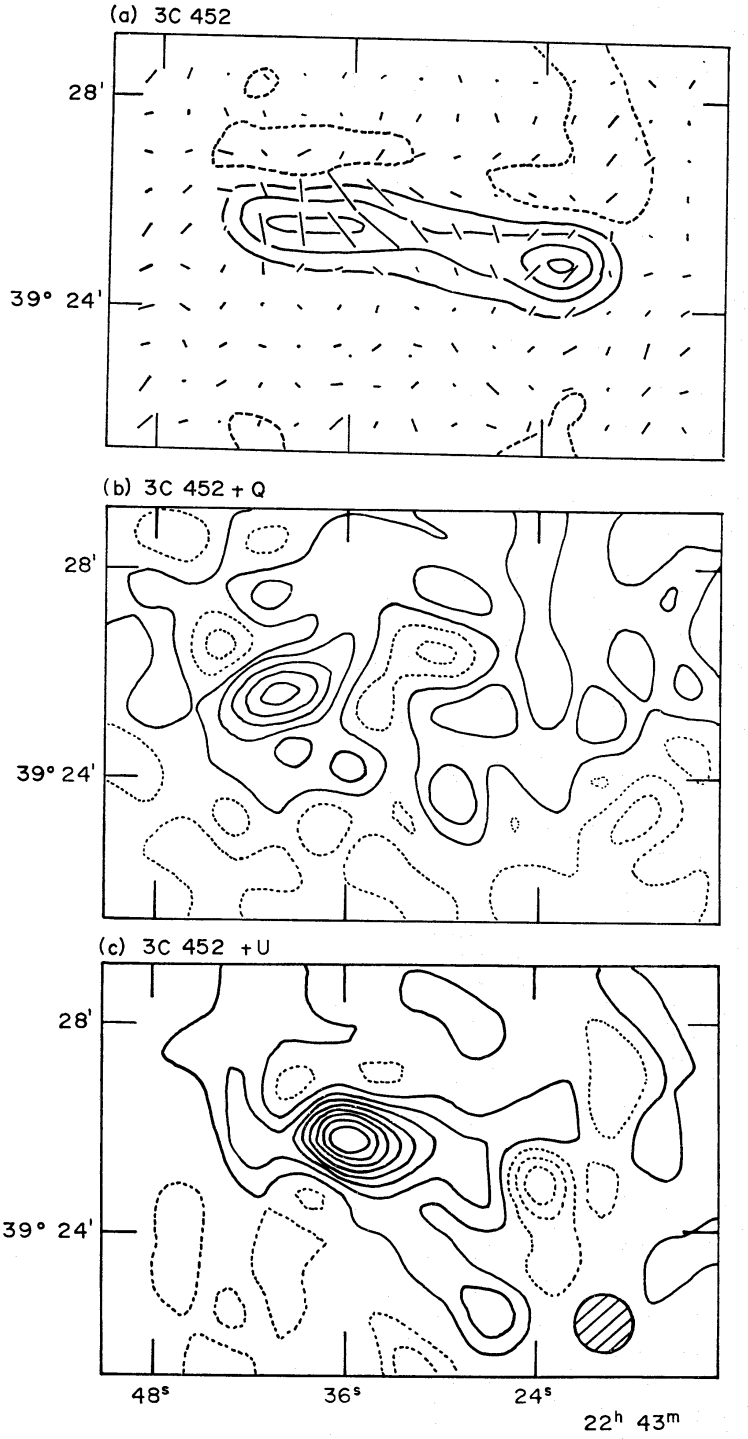

FIG. 5. 3C 452. (*a*) *Vectors of polarized flux superposed on contours of total intensity. The longest vector represents a polarized flux of* $0{\cdot}23 \times 10^{-26}$ *W m*$^{-2}$ *Hz*$^{-1}$ *(beam area)*$^{-1}$. *The contour interval is* $0{\cdot}25 \times 10^{-26}$ *W m*$^{-2}$ *Hz*$^{-1}$ *(beam area)*$^{-1}$. *Aerial coordinates.* (*b*) *and* (*c*) *Contours of Q and U respectively. The contour interval is* $2{\cdot}6 \times 10^{-28}$ *W m*$^{-2}$ *Hz*$^{-1}$ *(beam area)*$^{-1}$. *Aerial coordinates. The r.m.s. noise level is* 2×10^{-28} *W m*$^{-2}$ *Hz*$^{-1}$ *(beam area)*$^{-1}$.

TABLE IV

The net polarization of 3C 452 at different wavelengths

	λ (cm)	Polarization (per cent)	Position angle (°)
Kronberg & Conway (1970)	49·1	0·3 ± 0·3	5 ± 35
Bologna *et al.* (1969)	21·2	4·0 ± 0·5	24 ± 5
This paper	21·1	4·6 ± 0·5	32 ± 7
Seielstad & Weiler (1969)	21·1	3·9 ± 1·0	24 ± 3
Berge & Seielstad (1967)	18·0	7·0 ± 0·4	36 ± 2
Seielstad (1967)	10·6	8·4 ± 0·9	4 ± 4
Maltby & Seielstad (1966)	10·6	6·7 ± 1·5	17 ± 6
Sastry *et al.* (1967)	6	9·6 ± 0·3	126 ± 1

TABLE V

Polarization along major axis of 3C 452

	This paper (λ 21·1 cm)		Seielstad & Weiler (λ 21·2 cm)		Seielstad (λ 10·6 cm)	
α(1950·0)	%	p.a.	%	p.a.	%	p.a.
$22^h\ 43^m\ 18^s$	0 ± 2	—				
20^s	3 ± 1	135				
22^s	3 ± 1	135	2	147	9·3 ± 1·9	4 ± 8
24^s	5 ± 1	135				
26^s	0 ± 2	—				
28^s	5 ± 2	45	—	—	—	—
30^s	6 ± 2	45				
32^s	14 ± 2	45				
34^s	16 ± 1	50				
36^s	18 ± 1	45	8	25	7·7 ± 1·6	4 ± 8
38^s	12 ± 1	30				
40^s	9 ± 1	6				
42^s	—	—				
44^s	5 ± 2	22				

6.6 3C 461 (*Cas A*)

Maps of I, Q and U are shown in Fig. 6. The beam-width at the declination of this source is $47'' \times 55''$ arc so the resolution for the I map is lower than that achieved by Ryle, Elsmore & Neville (1965) at λ 21·3 cm and Rosenberg (1970) at λ 11·1 cm. No pencil-beam polarization observations, however, have previously been published with a comparable resolution. The polarization is found to be very low at all points and there is evidently strong depolarization between λ 1·55 cm and λ 21·3 cm. At the former wavelength Mayer & Hollinger (1968), with a 1′·7 arc pencil-beam, found a remarkably symmetrical distribution consistent with a uniform polarization of 7 per cent and a radial magnetic field.

The integrated polarization, determined from the maps of Q and U and from observations at small base-lines, is (0·2 ± 0·1) per cent in p.a. 90° ± 20° which may be compared with the value (0·11 ± 0·07) per cent in p.a. 116° ± 45° quoted by Seielstad & Weiler (1968). The former value, of course, depends upon the assumption that the net polarization of Cyg A is zero, as discussed in Section 5.

The errors for the U map are substantially higher than those for the Q map because of the way the instrumental corrections were made and, although we

have felt it worth reproducing the U map, we have little confidence in any of the individual features. The Q map is more satisfactory and there is good agreement between an east–west strip distribution derived from our map and that by Seielstad & Weiler (1968). This gives confidence in the reality of the weak $+Q$ feature at $\alpha = 23^h\ 21^m\ 34^s$, $\delta = 58^\circ\ 33'$ which may be of considerable significance since it lies immediately outside the well-known 'gap' in the Cas A shell (see e.g. Rosenberg 1970) and coincides with the optical filaments discussed by Minkowski (1966). Since this feature extends beyond the edge of the source on the I map, the percentage polarization may be very high but cannot be estimated with any accuracy.

The net polarization of Cas A is found to be low at all radio frequencies, but it is clear from the results of Mayer & Hollinger (1968) that, at high frequencies, this is due to averaging a radially symmetrical polarization distribution. The

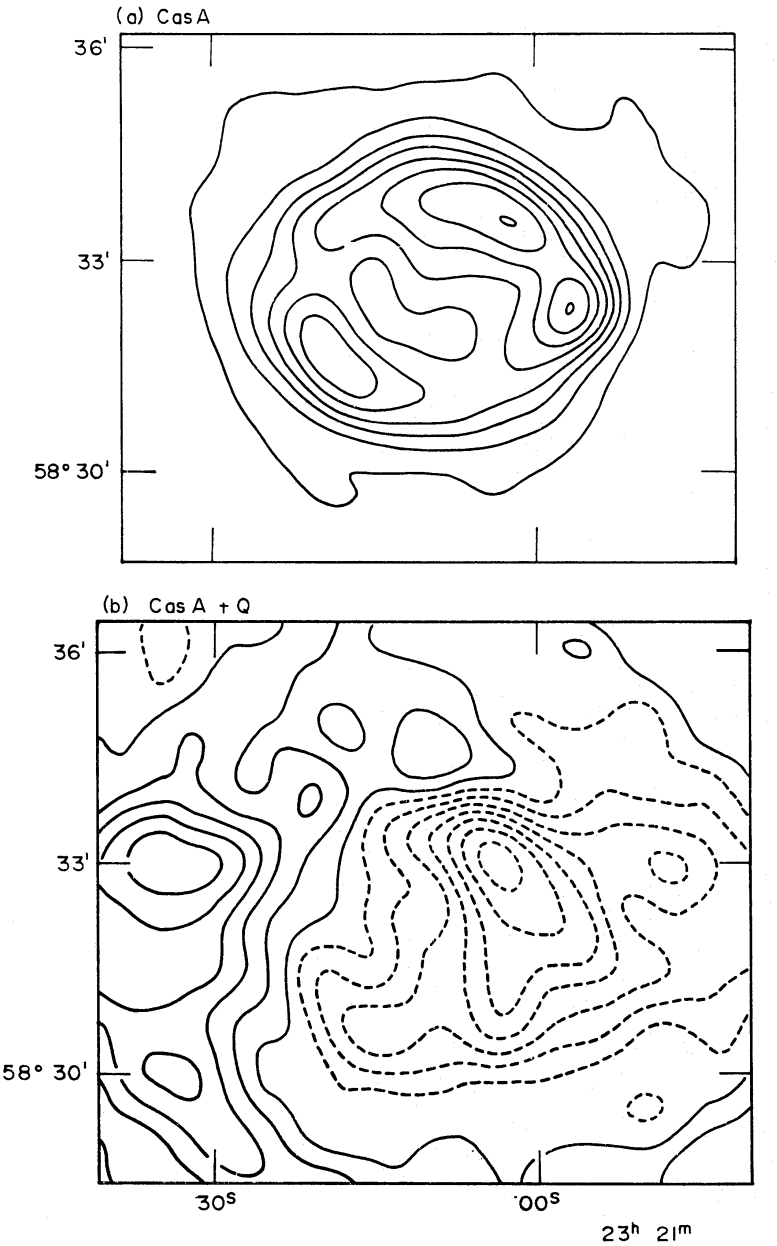

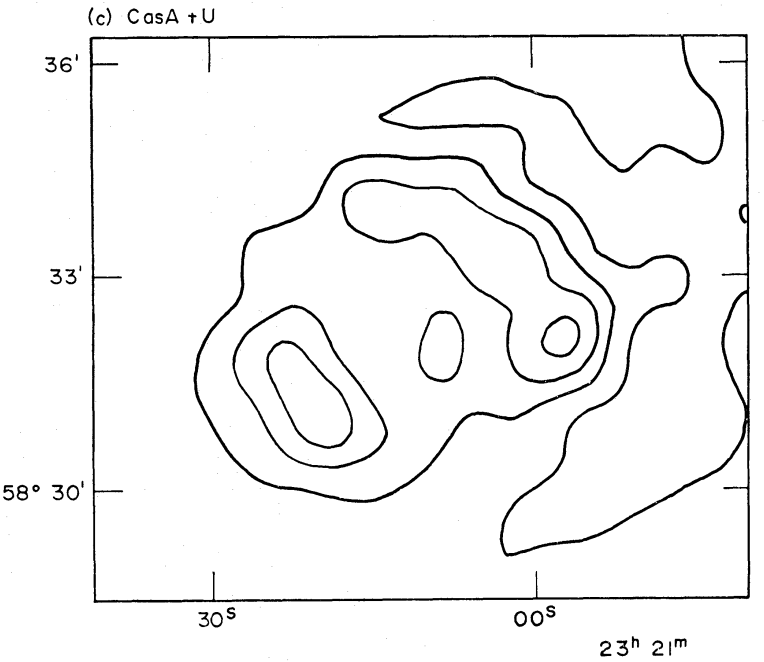

FIG. 6. 3C 461 (*Cas A*). (*a*) *Contours of* $I+U$. *The contour interval is* $22{\cdot}6\times10^{-26}$ *W* m^{-2} *Hz*$^{-1}$ (*beam area*)$^{-1}$. *Aerial coordinates.* (*b*) *Contours of Q. The contour interval is* $0{\cdot}065\times10^{-26}$ *W* m^{-2} *Hz*$^{-1}$ (*beam area*)$^{-1}$. *Aerial coordinates.* (*c*) *Contours of U. The contour interval is* $0{\cdot}14\times10^{-26}$ *W* m^{-2} *Hz*$^{-1}$ (*beam area*)$^{-1}$. *Aerial coordinates.*

strong depolarization from λ 1·55 cm to λ 21·1 cm for individual regions of the source is nevertheless a noteworthy feature. Rosenberg (1970) has discussed depolarization in relation to his λ 11-cm map in which he placed an upper limit of 2 per cent on the polarization of the major features. In an attempt to explain the low intensity of radiation from the centre of the source, he tested models with a radial magnetic field, as suggested by the results of Mayer & Hollinger (1968), but was unable to reconcile both the low central intensity and the low degree of polarization in the shell. He mentioned an alternative possibility for the field configuration, i.e. van der Laan's (1962) model in which the development of the supernova shell is influenced by the direction of the interstellar magnetic field. Whiteoak & Gardner (1968) attributed the low central brightness of a supernova remnant in Centaurus to this mechanism. If we suppose that the magnetic field around the shell of Cas A is indeed primarily along the line of sight, as required to explain the low central intensity, and take the values of the physical parameters as given in Section 4.6 of Rosenberg's paper, viz. $N_e\approx5$ cm^{-3} (assuming complete ionization), $B\approx5\times10^{-4}$ G and a shell radius ≈2 pc, then the internal Faraday rotation along a line of sight through the shell is ≈18 rad at λ 21·1 cm. This would seem to be adequate to account for the depolarization as due to internal Faraday dispersion (e.g. Burn 1966; Gardner & Whiteoak 1966).

ACKNOWLEDGMENTS

Many people have been involved with the building of the Half-Mile telescope and the reduction of the data. In particular we thank Professor Sir Martin Ryle for advice and encouragement, Donald Mackay for his interest in the construction

of the telescope, R. Atkins for developing the degenerate parametric amplifiers, Dr S. Kenderdine and Mrs E. M. Waldram for programming assistance and Mrs Barbara Petrie for her work on the data reduction. One of us (M. C. H. W.) gratefully acknowledges the receipt of a Science Research Council studentship and financial assistance from St John's College, Cambridge. The construction of the telescope was made possible by financial support from the Science Research Council.

Mullard Radio Astronomy Observatory, Cavendish Laboratory, Cambridge

REFERENCES

Baldwin, J. E., 1967. *I.A.U. Symposium* No. 31, 337.
Berge, G. L. & Seielstad, G. A., 1967. *Astrophys. J.*, **148**, 367.
Berge, G. L. & Seielstad, G. A., 1969. *Astrophys. J.*, **157**, 35.
Biraud, F., 1969. *Astr. Astrophys.*, **1**, 156.
Bologna, J. M., McClain, E. F. & Sloanaker, R. M., 1969. *Astrophys. J.*, **156**, 815.
Burn, B. J., 1966. *Mon. Not. R. astr. Soc.*, **133**, 67.
Cooper, B. F. C., Price, R. M. & Cole, D. J., 1965. *Aust. J. Phys.*, **18**, 589.
Dickel, J. R., 1969. *Astrophys. Lett.*, **4**, 109.
Elsmore, B., Kenderdine, S. & Ryle, M., 1966. *Mon. Not. R. astr. Soc.*, **134**, 87.
Fomalont, E. B., 1970. *Astrophys. J.*, **160**, L73.
Gardner, F. F. & Whiteoak, J. B., 1966. *A. Rev. Astr. Astrophys.*, **4**, 245.
Kerdemelidis, V., 1966. Calif. Inst. of Tech., Antenna Lab., Tech. Rep. No. 36.
Kronberg, P. P. & Conway, R. G., 1970. *Mon. Not. R. astr. Soc.*, **147**, 149.
Laan, H. van der, 1962. *Mon. Not. R. astr. Soc.*, **124**, 179.
Macdonald, G. H., Kenderdine, S. & Neville, A. C., 1968. *Mon. Not. R. astr. Soc.*, **138**, 259.
Mackay, C. D., 1969. *Mon. Not. R. astr. Soc.*, **145**, 31.
Maltby, P. & Seielstad, G. A., 1966. *Astrophys. J.*, **144**, 216.
Mayer, C. H. & Hollinger, J. P., 1968. *Astrophys. J.*, **151**, 53.
Minkowski, R., 1966. *Nature, Lond.*, **207**, 740.
Mitton, S. A., 1970. *Astrophys. Lett.*, in press.
Morris, D. & Berge, G. L., 1964. *Astr. J.*, **69**, 641.
Morris, D., Radhakrishnan, V. & Seielstad, G. A., 1964. *Astrophys. J.*, **139**, 551.
Rosenberg, I., 1970. *Mon. Not. R. astr. Soc.*, **147**, 215.
Ryle, M., Elsmore, B. & Neville, A. C., 1965. *Nature, Lond.*, **205**, 1259.
Sastry, C. V., Pauliny-Toth, I. I. K. & Kellermann, K. I., 1967. *Astr. J.*, **72**, 230.
Seielstad, G. A., 1967. *Astrophys. J.*, **147**, 24.
Seielstad, G. A., 1969a. Paper presented at U.R.S.I. XVIth General Assembly, Ottawa.
Seielstad, G. A., 1969b. *Astr. Astrophys.*, **2**, 372.
Seielstad, G. A. & Weiler, K. W., 1968. *Astrophys. J.*, **154**, 817.
Seielstad, G. A. & Weiler, K. W., 1969. *Astrophys. J. Suppl.*, **18**, 85.
Whiteoak, J. B. & Gardner, F. F., 1968. *Astrophys. J.*, **154**, 807.
Wright, M. C. H., 1970. *Mon. Not. R. astr. Soc.*, **150**, 271.